



HOW ANTIARRHYTHMIC DRUGS INCREASE THE RATE OF SUDDEN CARDIAC DEATH

C. FRANK STARMER

Medical University of South Carolina, Charleston, SC 29425, USA
starmarf@musc.edu

Received January 10, 1998; Revised October 18, 2001

Two large clinical trials of drugs that exhibited significant antiarrhythmic properties in single cells were found to increase the rate of sudden cardiac death in patients by two to three fold over untreated patients. We hypothesized that premature excitation within the drug-altered vulnerable region, a region that trails each excitation wave, might be one mechanism for initiating re-entrant tachyarrhythmias that could lead to ventricular fibrillation and sudden cardiac death. With numerical studies of a cardiac cell model, we probed the determinants of the vulnerable period. We found that antiarrhythmic drugs that block the sodium channel can increase the duration of the cardiac vulnerable period by both slowing conduction velocity and reducing the gradient of excitability. Coupling the dynamics of drug binding to ion channels with wave formation in a nonlinear excitable medium provides new insights into possible arrhythmogenic mechanisms.

Keywords: Nonlinear dynamics; antiarrhythmic drugs; vulnerable window; use-dependent; cardiac model; re-entry; proarrhythmic.

1. Introduction

“In few specialties of medicine are new promising drugs shown to be so much inferior to placebo and, even worse, to increase mortality,” wrote Prof. John Sanderson in an editorial discussing the unexpected and disappointing results of yet another large scale clinical trial of cardiac antiarrhythmic drugs [Sanderson, 1996]. Until recently, clinicians thought that depressing the response to an unexpected excitation of the heart (PVC or premature ventricular contraction) would reduce the incidence of arrhythmias leading to sudden cardiac death. Sanderson’s paradox was that new antiarrhythmic drugs, able to extend the refractory period in isolated cells, actually increased the rate of sudden cardiac death observed in clinical trials, in spite of the fact that $> 80\%$ of the responses to unexpected endogenous excitations of the heart were suppressed [CAST Investigators, 1989; CAST II Investigators,

1992]. Is there a specific mechanism that links cellular antiarrhythmic effects (suppression of a high percentage of unexpected excitatory events) with multicellular proarrhythmic effects (increased incidence of sustained spiral wave activity)?

Potentially fatal cardiac arrhythmias arise from unexpected stimuli or PVCs [Allessie *et al.*, 1973; Krinsky, 1966]. For example, stress, vigorous exercise or a heart attack can alter the cellular environment in the heart, leading to spontaneous oscillation of otherwise quiescent cells. If the amplitude of the oscillation is sufficient to excite neighboring cells, then either a continuous wave or a wave fragment will form depending on the state of neighboring cells (some can be in the rest state while others might be in the refractory state). A continuous wave propagates in all directions away from the excitation site and eventually is extinguished by colliding with itself. On the other hand, a wave fragment or wavelet, formed by successful propagation

in some directions and failed propagation in other directions, can evolve into a spiral wave. Since a spiral wave is self-sustaining, a pattern of re-excitation evolves that can lead to loss of mechanical pumping, reduced blood pressure and possibly death.

A standard clinical paradigm for managing patients with a predisposition to serious cardiac rhythm disturbances has been to reduce the likelihood of aberrant excitation. This was accomplished by treating patients with drugs (ion channel blockers) that either amplified the requirements to excite individual cardiac cells (by blocking Na channels) or prolonged the period of time a cell was inexcitable (by blocking K channels).

The paradox articulated by Sanderson was that all drugs tested in two major recent clinical trials [CAST Investigators, 1989; CAST II Investigators, 1992] significantly prolonged refractoriness in studies of isolated cells. During clinical trials, though, treated patients died from sudden cardiac death at a rate two to three times that of the untreated groups. The purpose of this paper is to explore how antiarrhythmic drugs might facilitate initiation of potentially life threatening arrhythmias. As stated above, wavelets can be initiated by excitation within a vulnerable region of the heart. Consequently, we explored the determinants of the vulnerable region (VR), first articulated by Wiener and Rosenblueth [1946] and the role Na channel availability played in the dynamics of front formation. The extent of the VR was sensitive to both the velocity of the parent wave and the gradient of excitability at the point of excitation. More important, we found that slowly unbinding antiarrhythmic drugs reduced the gradient of excitability, thus extending the VR.

2. Numerical Methods

Although there are many models available to explore numerically the behavior of an excitable cell, we chose the Beeler–Reuter (BR) [1977] model in order to avoid the complexities introduced by activation of numerous ion channels included in more realistic cardiac models [Luo & Rudy, 1991]. The behaviors that we explore in this paper (threshold of excitation, front formation, front collapse, unidirectional conduction) are generic properties of all excitable media and are determined by net directional flow of transmembrane currents. Consequently, even the two current model of FitzHugh and Nagumo [1961] is suitable for exploring mech-

anisms associated with refractory and vulnerable regions.

The excitable cell model used in our studies was based on a parallel circuit composed of a membrane capacitance and several gated ion channels that permit flow of ions between the extracellular and intracellular spaces [Hodgkin & Huxley, 1952; Beeler & Reuter, 1977] and is expressed as:

$$C_m \frac{\partial V}{\partial t} = \frac{1}{R_i} \nabla^2 V - I_{\text{ion}} \quad (1)$$

where R_i is the internal resistivity of the cell, and the ionic currents, I_{ion} are defined in terms of gated conductances of the form

$$I_{\text{ion}} = g_{\text{ion}} a_{\text{gate}} d_{\text{gate}} (V - V_{\text{ion}}) \quad (2)$$

where g_{ion} is the maximum ensemble conductance, a_{gate} and d_{gate} represent the fractions of open activation and inactivation gates and V_{ion} is the reversal potential for the channel charge carrier. The channel gating variables vary between 0 (closed) and 1 (open) and are modeled in terms of a first-order transition between closed and open states [Hodgkin & Huxley, 1952]:



The dynamics are described by

$$\frac{da}{dt} = \alpha_a(V)(1 - a) - \beta_a(V)a \quad (4)$$

where $\alpha(V)$ and $\beta(V)$ are voltage sensitive transition rates and a is the fraction of open channels.

Propagation depends on the relationship between the source of charge available to diffuse into neighboring cells and the charge required by neighboring cells to exceed the threshold of excitation. Here we will focus on the Na current and factors that modulate its magnitude and write the reaction–diffusion equation as:

$$C_m \frac{\partial V}{\partial t} = \frac{1}{R_i} \nabla^2 V - (g_{\text{Na}} m^3 h j (V - V_{\text{Na}}) + I_{\text{other ion}}) \quad (5)$$

where g_{Na} is the maximum Na conductance, m^3 is the fraction of open activation gates and h and j are the fractions of open fast and slow inactivation gates. For our analysis, we approximate excitability in terms of the density of Na channels available to open upon excitation, i.e. Availability = $A = g_{\text{Na}} h j$.

A cable was constructed by linking excitable segments with an axial resistivity of 250 ohm-cm and a cell radius of 7 microns. The cable equation was discretized with space steps of 1/512 cm and time steps 1/128 ms. The discretized equations were solved using an implicit method. The boundary conditions at the cable ends were nonconducting, i.e. $\partial V/\partial x = 0$.

We measured the vulnerable period (VP) in a 10 cm 1D cable using a conditioning wave followed by a test stimulus. We initiated a conditioning wave at the left boundary of the cable (see Fig. 6 top) with current injection ($-10 \mu\text{A}/\text{cm}^2$). We probed the post-refractory interval with test stimuli at a site 2.5 cm from the left end of the cable by injecting $-10 \mu\text{A}/\text{cm}^2$ for 0.25 ms. For studies of the VP dependence on electrode length, the test stimuli were produced by injecting a near-threshold current ($-1 \mu\text{A}/\text{cm}^2$ for 0.25 ms) into a test electrode with lengths varying from 1.5 to 3.9 mm. The VP was located by using a binary search of the time window

bounded by the refractory period and the return to full excitability following the passage of the conditioning wave.

3. Cardiac Cell Model

Under normal conditions, excitable cells exhibit a stable resting state and an unstable excited state. With low amplitude stimuli, there is no response, but with stimuli that exceed a certain threshold, the cell's electrical potential makes a major departure from equilibrium generating an action potential shown in Fig. 1.

To visualize the dynamics of channel gating, we computed a typical cardiac action potential (Fig. 2) and plotted the time course of the sodium channel activation gate (m), the fast inactivation gate (h) and the slow inactivation gate (j). At the rest potential, the activation gate, $m = 0$, and the fast and slow inactivation gates (h and j) are open ($h = j = 1$). Immediately after stimulation the

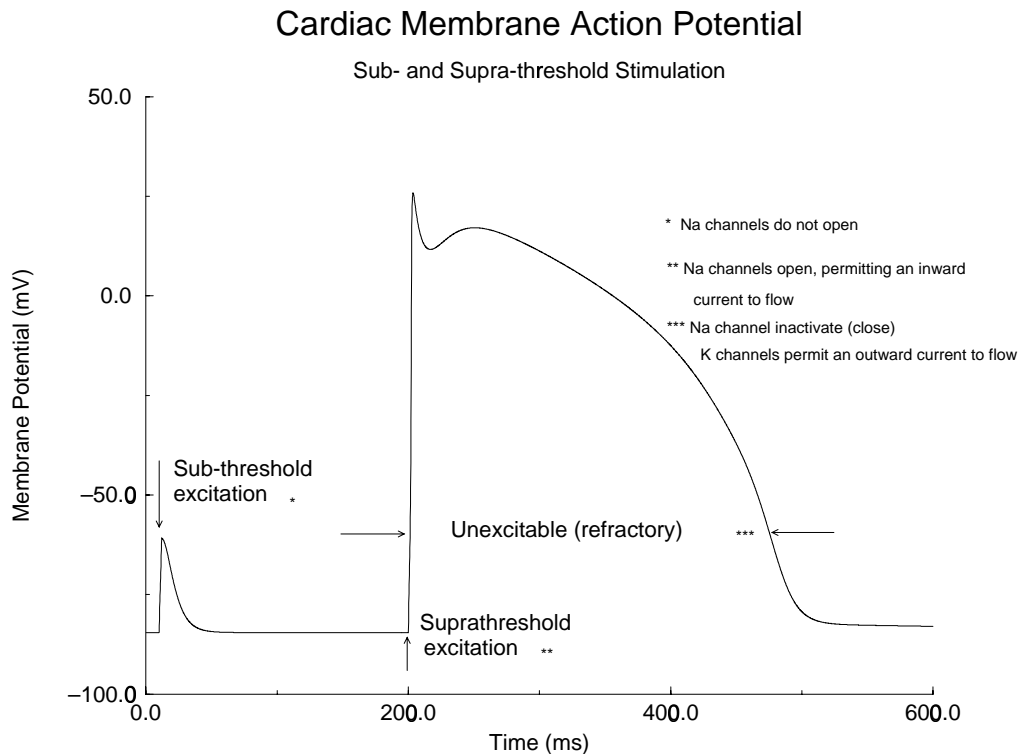


Fig. 1. The computed action potential following subthreshold and suprathreshold stimulation. A subthreshold current was applied at $t = 10$ ms and was insufficient to raise the transmembrane potential above the threshold for opening Na channel activation (m) gates. Following suprathreshold stimulation at $t = 200$ ms a sufficient number of Na channels opened such that the influx of Na current continued to depolarize the membrane. Inactivation of Na channels terminates current flow within 1 ms. On a slower time scale, voltage sensitive K channels open (permitting a small outward current) and Ca channels open (permitting a small inward current). The result is a net outward current which gradually repolarizes the membrane, returning the potential to the rest value.

Cardiac Action Potential and Gating

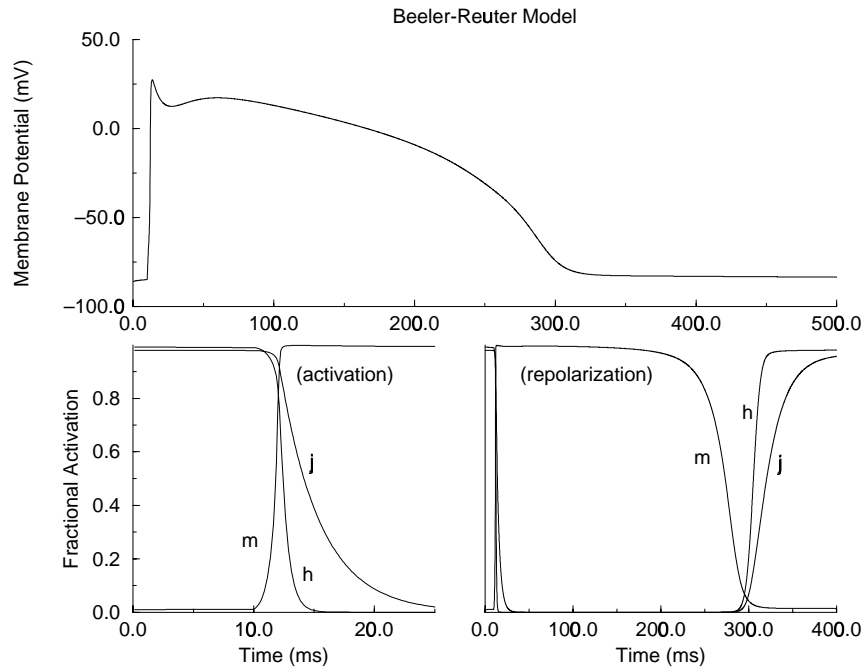


Fig. 2. A computed cardiac action potential and channel gating. Shown in the lower panels are the time course of the activation gate (m) and the fast and slow inactivation gates (h and j). At the rest potential, the m gate is closed ($m = 0$) while the inactivation gates are open ($h = j = 1$). Following excitation, the membrane depolarizes and the activation gate rapidly changes from a closed to an open configuration ($m > 0$). On a slower time course, the inactivation gates change from open to closed ($h, j < 1$). The composite gating behavior creates a time varying conductance: $g_{Na} = m^3 h j$ which rapidly increases and then more slowly returns to zero. The two lower panels display gating dynamics during the excitatory phase of the action potential (at $t = 10$ ms) and during repolarization (at $t = 300$ ms).

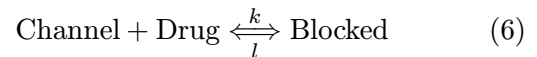
fraction of open m gates increases rapidly while the fraction of open inactivation gates (h and j) decrease on a slower rate. In cardiac cells, the relatively slow inactivation process, which terminates conduction, is responsible for the refractory period, an interval of time during which the cell remains unresponsive to stimulation. Due to the voltage sensitivity of the inactivation rate constants, recovery from inactivation typically does not occur until the membrane potential is within 10–15 mV of the rest potential.

Action potentials are initiated by stimulation that facilitates opening of channels carrying a depolarizing current. As channel gates open, ionic currents flow down their concentration gradient. Following excitation, membrane depolarization proceeds by the inward flow of Na (or Ca) ions through Na (or Ca) channels. On a slower time course, potassium channels begin to open, initiating membrane repolarization by the outward flow of K ions. As the membrane potential repolarizes, the Na channel gates revert to their rest configuration: the activation gates close while the inactivation gates

open (but on a time scale roughly ten times slower than the activation time scale). Recovery from channel inactivation terminates the period of refractoriness. At the rest potential (about -84 mV), the fraction of inactivated Na channels is essentially zero, i.e. $h = j = 1$, and the cell is maximally excitable.

4. Modeling the Drug-Channel Interaction

Many interactions between drugs and ion channels are interesting because the chemistry of these interactions departs from traditional “continuous” chemistry. In continuous chemical reactions, when one mixes two chemical reagents, each component has continuous access to each other and the reaction proceeds at a constant rate and is schematically represented by



Let $b(t)$ represent the fraction of drug-complexed channels, then the time-dependent

fraction of drug-complexed channels is described by:

$$\frac{db}{dt} = k[\text{Drug}](1 - b) - lb \quad (7)$$

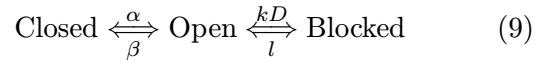
where k and l are forward and reverse rate constants. The time course of binding is described by:

$$b(t) = b(\infty) + [b(0) - b(\infty)]e^{-(k[\text{Drug}] + l)t} \quad (8)$$

Early studies of antiarrhythmic drugs, though, revealed that in the presence of an antiarrhythmic drug, the rate of rise of the cellular action potential was reduced as the rate of stimulation was increased. This observation was consistent with a transient reduction in Na conductance and suggested that membrane excitability was in some manner dependent on the rate of stimulation [Johnson & McKinnon, 1957; Heistracher, 1971]. More recent voltage-clamp studies of cardiac cells revealed that the altered excitability was due to transient blockade of the Na channel by the drug molecule [Gilliam *et al.*, 1989; Starmer *et al.*, 1991; Zilberter *et al.*, 1994].

The frequency-dependent pattern of channel blockade was modeled by postulating that the drug must selectively bind to one of the states of a channel: either rest, open or inactivated [Starmer &

Grant, 1985; Starmer, 1988] as shown in Fig. 3. We captured the state dependence of channel blockade by adding a blocked state to the channel gate transition model. Blockade of an activated channel was thus described by:



Let b represent the fraction of blocked channels, m represent the fraction of open channels, c represent the fraction of closed channels and D represent the drug concentration, k and l represent the rates of block and unblock. From conservation of channels: $c + m + b = 1$ and we can write the differential equations characterizing the blocking process as

$$\frac{db}{dt} = k[D]m - lb \quad (10)$$

$$\frac{dm}{dt} = \alpha(1 - m - b) + lb - (\beta + kD)m \quad (11)$$

For most drug-channel reactions, the rates of drug binding and unbinding are slow compared with the voltage-dependent transition rates between open and closed channel conformations. Assuming rapid

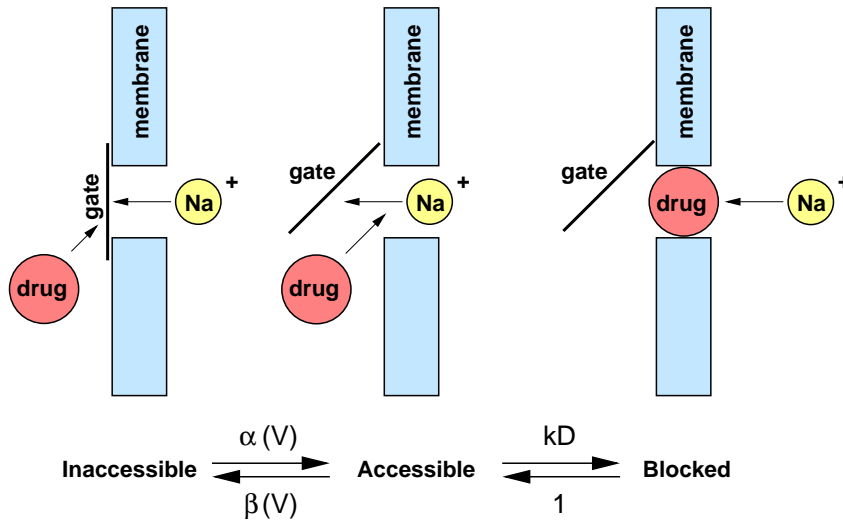


Fig. 3. A simple model of ion channel blockade. Shown is the cell membrane and a single sodium ion channel. The channel is in one of three conformations: either the binding site is inaccessible (left), accessible but unblocked (middle) or accessible and blocked (right). The channel gate is sensitive to the transmembrane potential, controls the flow of ions through the channel and is either closed (left) or open (middle and right). We hypothesize that the gating process also controls access to the drug binding site. As shown, when the gate is in the closed configuration the diffusion path to the binding site is blocked. When the gate is in the open configuration, the diffusion path is unrestricted and the drug is free to migrate to the binding site and possibly form a drug-complexed (blocked) channel (right). Drug-complexed channels do not conduct. When the gating transitions are rapid compared with the time constant of drug binding, then Eq. (12) accurately describes the time course of the blockade process as a function of the rates of binding and unbinding as well as the voltage sensitive gate transition rates, α and β .

equilibrium between the closed and open states, Eq. (4) reduces to $\alpha(1-m) = \beta m$ or $m = \alpha/(\alpha + \beta)$ so that the blockade equation can be rewritten as

$$\frac{db}{dt} = \frac{\alpha}{\alpha + \beta} k[D](1-b) - lb \quad (12)$$

The voltage-sensitive gating rate constants, α and β , thus modulate the rate of formation of drug complexed channels, $k[D]$. Because the channel gating transition rates α and β are sensitive to membrane potential, the diffusion path of drug to the binding site is modulated by membrane potential. At depolarized potentials (i.e. during the action potential) $\alpha \gg \beta$, thus promoting drug-channel interactions. At the rest potential, $\alpha \ll \beta$, thus inhibiting binding. During periodic stimulation, when the interval between successive action potentials is greater than $4/l$, there is no net accumulation of blocked channels. However, when the recovery interval is less than $4/l$, there is a net increase in blocked channels [see Figs. 4 and 5(b)].

To explore the dynamic effects of use-dependent drug-channel interactions, we augmented the membrane models [Beeler & Reuter, 1977] with equations similar to Eq. (12) that describe the gate control of the drug diffusion path. When the inactivation gate (h or j) is assumed to control binding site access, the blockade equation (inactivation state blockade) was written as:

$$\frac{db}{dt} = k[D](1-h)(1-b) - lb \quad (13)$$

Similarly, when the fraction of open channels is assumed to control binding site access, the kinetics are described by:

$$\frac{db}{dt} = k[D]m^3hj(1-b) - lb \quad (14)$$

With either blockade model, the sodium conductance and hence, excitability, was reduced by the fraction of blocked channels. The macroscopic Na conductance in the presence of drug is represented by $g_{Na}hj(1-b)$. The Na current is now described by:

$$I_{Na} = g_{Na}m^3hj(1-b)(V - V_{Na}) \quad (15)$$

We approximated cellular excitability in terms of the Na channels available for transition from the rest state to the activated state: Availability = $g_{Na}(1-b)hj$.

Use- and frequency-dependent blockade are readily demonstrated with this model. With pulse

Use- and Frequency-Dependent Channel Blockade

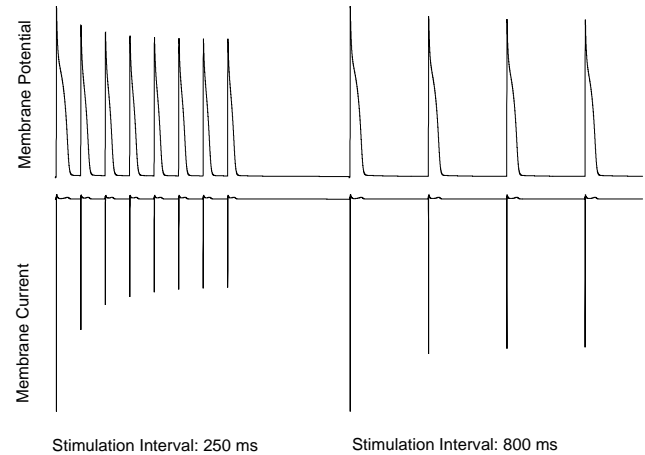


Fig. 4. Repetitive stimulation of cardiac displays “use- and frequency-dependence”. The top trace is a sequence of computed action potentials using the Beeler–Reuter model augmented by Eqs. (12) and (14) and stimulated with a 4 Hz pulse train (left) and a 1.25 Hz pulse train (right). The calcium conductance (g_{Ca}) was reduced to 0.045 (from the standard BR value of 0.09) in order to reduce the action potential duration. The rates of binding (kD) and unbinding (l) were 4/s and 1/s respectively. The bottom trace displays the total membrane current. During an action potential, the channels switch between different configurations that alter accessibility of the drug binding site. Here we depict open channel block where the open channel permits diffusion of drug to the binding site. Consequently, formation of drug-complexed channels can only take place when the channel is open. Similarly, some drugs can only block inactivated channels as if the inactivation gate controls access to the binding site.

train stimulation, we computed cellular action potentials and total membrane current for two stimulation frequencies. That reduction in the recovery time enhances the accumulated block is readily seen when comparing results associated with 250 ms stimulus intervals (Fig. 3, left) with 800 ms stimulus intervals (Fig. 3, right).

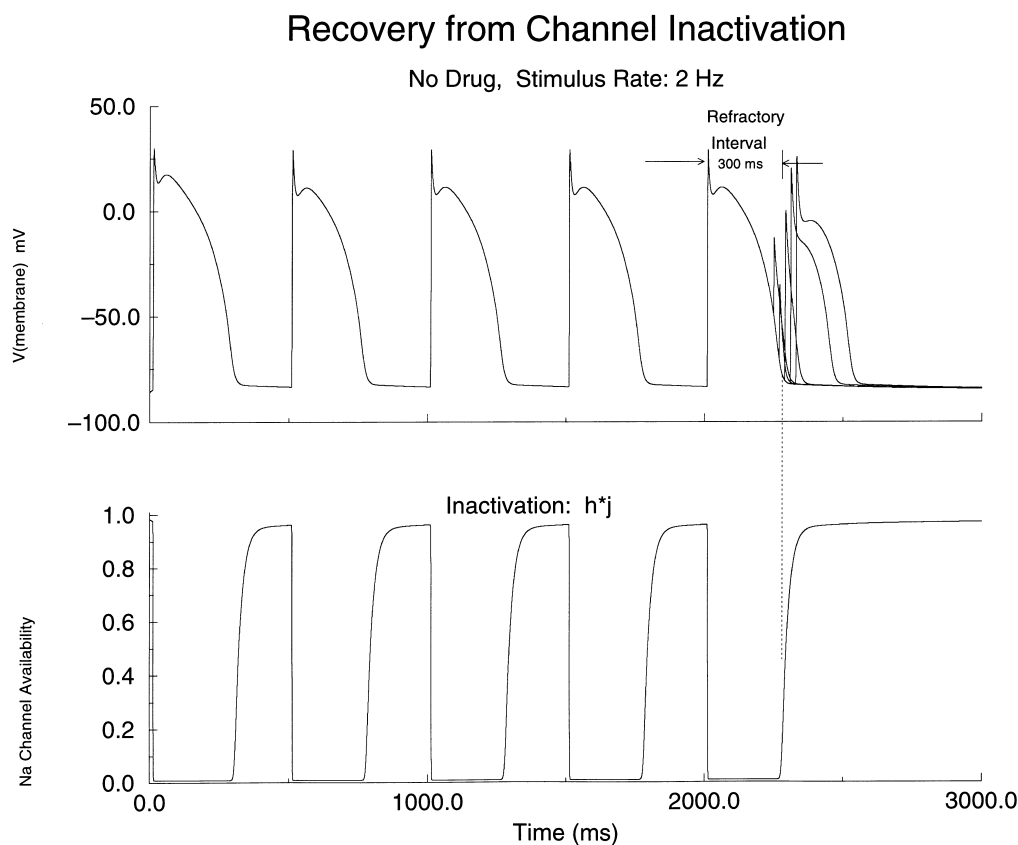
In summary, we extended the BR model equations with Eqs. (13) or (14), depending on the blockade process, and substituted Eq. (15) for the Na current. The validity of this approach has been tested with cellular studies of both open channel and inactivated blockade. We found good agreement, over a wide range of stimulus frequencies and drug concentrations, between observed blockade and model-based predictions of the time and frequency-dependent interaction of drugs with either inactivated or the open Na channels [Gilliam *et al.*, 1989; Starmer *et al.*, 1991a; Whitcomb *et al.*, 1989; Zilberter *et al.*, 1994].

5. Drug Alteration of Single Cell Responses to Stimulation

Until recently, the clinical paradigm for managing cardiac rhythm disturbances was to reduce cellular excitability either by using Na channel blocking drugs to prolong the refractory period or by using K channel blocking drugs to prolong the action potential duration. It had been thought that by prolonging the refractory period of a cardiac cell, either with Na or K channel blockade, the number of unexpected extra stimuli (PVCs arising from cells that decide to suddenly switch from a stable mode to an oscillatory mode) would be diminished thereby reducing the number of episodes of

potentially fatal rhythm disturbances. As clinical trials have demonstrated, therapy based on ion channel blockade was successful in reducing the number of unexpected extra stimuli but actually increased the number of fatal rhythm disturbances. To explore the nature of this paradox, we first investigated single cell responses to stimulation (where these drugs display their antiarrhythmic properties) and then probed multicellular responses to stimulation and subsequent front formation (where the drugs display their proarrhythmic properties).

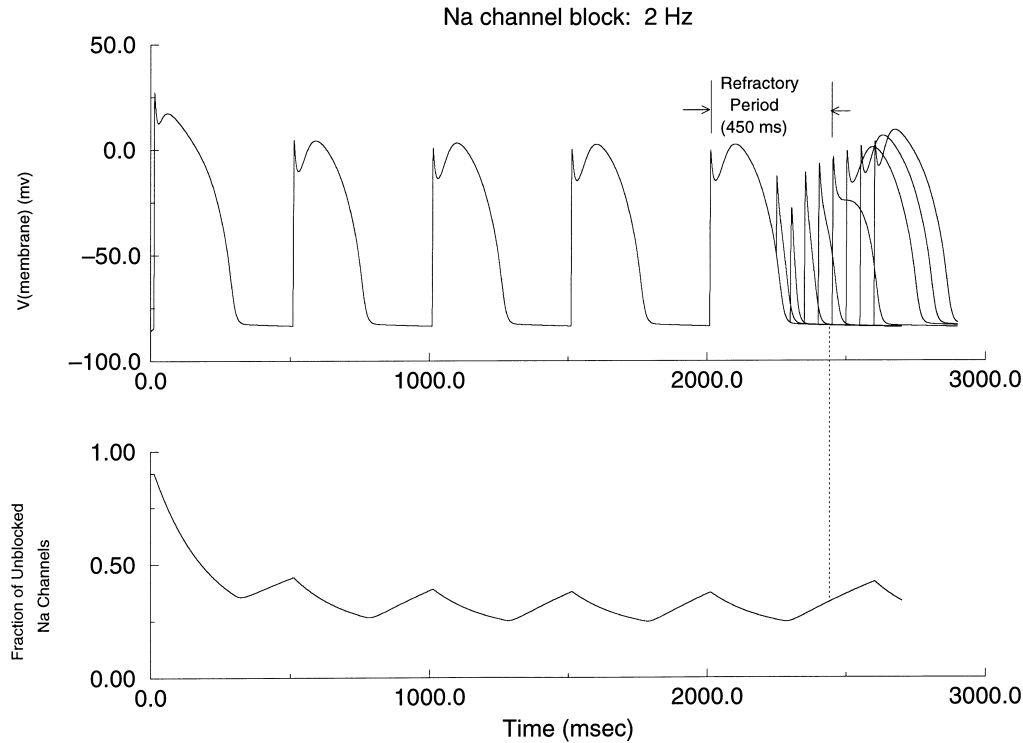
The refractory period and its modulation by drugs were readily demonstrated with paired stimuli (a conditioning stimulus, s1, followed after some delay by a test stimulus, s2). Figure 5 illustrates



(a)

Fig. 5. Periodic stimulation and the refractory period of a single cell. Shown in (a) is a train of action potentials (upper trace) initiated in response to a 2 Hz train of 5 s1 pulses followed by a test pulse (s2) under drug free conditions. The lower trace displays the fraction of available (noninactivated) Na channels ($h * j$) where h and j are the BR fast and slow inactivation variables. The cell was refractory when the s1–s2 delay was less than 300 msec. (b) illustrates the effect of a drug. For these studies we assumed blockade of inactivated channels with $kD = 4/\text{sec}$ and $l = 1/\text{sec}$. The upper trace shows the action potentials associated with the 2 Hz train of stimuli while the lower trace shows the use-dependent fraction of unblocked channels. Since the fraction of available channels is proportional to $h * j * (1 - b)$, and $h * j$ is approximately 1, the bottom trace indirectly reflects excitability, i.e. a large fractional block results in a poorly excitable preparation. The large fraction of blocked channels after the fifth stimulus pulse extended the refractory period to 450 msec.

Recovery from Channel Blockade



(b)

Fig. 5. (Continued)

the refractory period for a single cell in the absence of drug (a) and in the presence of a use-dependent drug that blocks inactivated channels (b). In (a), a train of five conditioning (s1) stimuli (2 Hz) was used to establish a steady state. Following the fifth pulse, a test (s2) stimulus ($1.5 \times$ threshold) was used to assess the excitability of the cell. When the delay between the last conditioning pulse (s1) and the test pulse (s2) was < 300 ms, the membrane was unable to initiate a new action potential. For s1–s2 delays > 300 ms, there was greater Na channel availability since more channels had recovered from inactivation. Consequently action potentials of increasing duration (in proportion to the s1–s2 delay) were initiated.

The refractory period was extended beyond the end of the action potential by periodic blockade of the Na channels as shown in Fig. 5(b). In the presence of a use-dependent drug, the refractory period was determined by the time required for Na channel availability ($hj(1 - b)$) to recover sufficiently to support initiation of a new action potential. A 2 Hz train of five pulses was used to establish a

steady-state pattern of channel blockade as seen in the lower panel. Using the s1–s2 stimulation protocol, the refractory period was extended to 450 ms thereby reducing the period of susceptibility to premature stimulation to 50 ms.

6. Vulnerability: A Multicellular Response

Ferris *et al.* [1936] and later, Wiggers and Wegria [1939] observed that ventricular fibrillation could be readily induced by stimulating a heart during an interval they called the vulnerable phase. As shown above [Fig. 5(b)], use-dependent Na blockade displayed antiarrhythmic properties by extending the refractory period secondary to a periodic reduction of the number of Na channels available to generate a new action potential [Johnson & McKinnon, 1957; Heistracher, 1971; Gilliam *et al.*, 1989]. In patients, though, use-dependent Na blockade increased the probability of spontaneous initiation of re-entrant arrhythmias that led to sudden cardiac death [CAST Investigators, 1989; CAST II Investigators, 1992].

Krinsky [1966] proposed that ventricular fibrillation could be linked to spiral waves of cardiac activation which could be initiated by stimulation within the vulnerable region. Utilizing the traveling boundary separating excitable and refractory cells that follows a propagating wave, Wiener and Rosenblueth [1946] proposed a model for the vulnerable period, an interval within which stimulation would lead to wavelet formation (a wave fragment). The W-R model of the vulnerable period depended on the velocity of the wave leading us [Starmer *et al.*, 1991b; Starmer *et al.*, 1994] to hypothesize that Na channel blockade would increase the cardiac vulnerable period and increase the likelihood of initiating a unidirectionally propagating wave (in 1D) or wavelets capable of evolving into spiral waves (in 2D).

The combined effect of an increase in the refractory interval and an increase in the vulnerable period will increase the probability that a randomly timed stimulus can trigger events leading to a re-entrant arrhythmia. Let RR be the interval between successive heart beats, RP be the refractory period and VP be the vulnerable period. Then $P(\text{arrhythmia}) = VP / (RR - RP)$. This ratio increases with either a prolonged refractory period or with a prolonged vulnerable period, or both. Given this direct link between likelihoods for triggering re-entrant arrhythmias by altering the RP and VP, we probed the vulnerable period to determine its sensitivity to Na channel availability, use-dependent channel blockade and electrode configuration.

Figure 6 illustrates a typical numerical experiment demonstrating formation of a unidirectionally propagating wave front by timing stimuli to occur within the vulnerable period. Shown at the top of the figure is the experimental setup: a length of excitable cable with two stimulation sites, s1 which is used to initiate a conditioning wave and s2 which is used to probe for the vulnerable period. For the 1D case, the vulnerable period was defined as the range of delays between the s1 and s2 stimuli that resulted in a unidirectional propagation. Shown are two conditions, the top is considered normal, with a maximum Na = conductance of 5 mS/cm² and the lower is considered diseased where the maximum Na conductance is reduced to 2 mS/cm². Each of the four panels shows the fate of a stimulus introduced at the s2 site. The time between each successive trace is 5 ms.

With a Na conductance of 5 mS/cm² (top sequence), a wave was initiated at the left bound-

ary and propagated from left to right. At an s1-s2 delay of 483.3 ms, the stimulus at the s2 site ignited a region that collapsed as shown by the traces at 5 ms intervals [Fig. 6(A)]. Delaying the s2 stimulus by 0.1 ms resulted in an ignited region that expanded in the retrograde direction and collapsed in the antegrade direction (unidirectional conduction) [Fig. 6(B)]. With an s1-s2 delay of 485.4 ms, the ignited region expanded in both directions [bidirectional conduction, Fig. 6(D)]. The VP was 1.9 ms and, assuming a uniform distribution of PVCs, then for a heart rate of 75 (interbeat interval of 800 ms), $P(\text{arrhythmia}) = 1.9 / (800 - 483.3) = 0.004$. When the Na conductance is reduced by 60% to 2 mS/cm², the conduction velocity of the s1 front slowed from 64.3 cm/sec to 31.7 cm/sec [Figs. 6(E)-6(H)], the refractory period increased from 483.3 ms to 554.5 ms and the VP increased from 1.9 ms to 22.3 ms. Thus under conditions of low excitability the $P(\text{arrhythmia}) = 22.3 / (800 - 554.5) = 0.09$, an approximately 20 fold increase compared with the normal or control value.

In addition to the demonstrating asymmetric front development resulting from stimulation within the vulnerable period, the two conditions [Figs. 6(A)-6(D) and Figs. 6(E)-6(H)] display differences in the transition from unidirectional to bidirectional conduction. Figure 6(C) shows a rapid collapse of the developing antegrade wave while Fig. 6(D) displays an immediate transition to incremental conduction. On the other hand Fig. 6(G) shows a very slow collapse of the developing antegrade wave and 6(H) shows a very slow transition from decremental to incremental conduction. The differences in these transition dynamics suggest that the vulnerable region is sensitive to medium excitability.

Wiener and Rosenblueth [1946] viewed the vulnerable region as determined by the movement of the transition point between refractory and excitable mediums. Traveling with each wave of excitation is a phase wave of excitability. Within this wave is a point that represents the transition from refractory (unexcitable) to excitable medium. Winfree [1987] realized that the transit of this point across the stimulus field would define a period of vulnerability and defined the VP as the ratio of the length of the stimulus field (L) to the wave velocity (v).

We tested the predicted linear relationships ($VP = L/v$) between the VP and electrode length and between VP and $1/\text{velocity}$ and found good

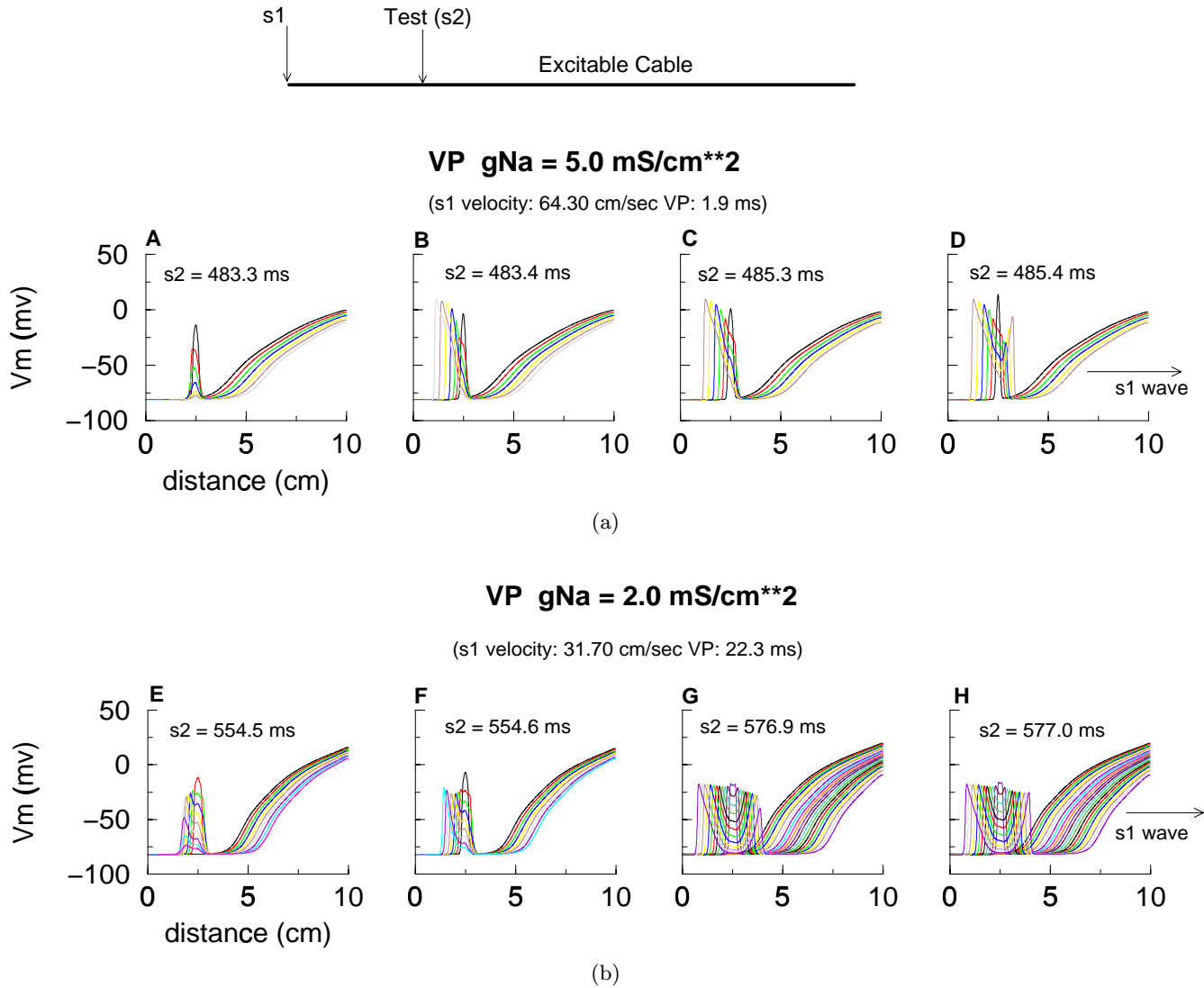


Fig. 6. Demonstration of the vulnerable period. Using a 10 cm cable, a conditioning wave was initiated (s1) at the left end of the cable. A test wave was initiated (s2) at a location 2.5 cm to the right of the conditioning site. Shown are spatial distributions (expanding away from the stimulation site) of the membrane potential plotted at 5 ms intervals. Varying the s1-s2 delay reveals the boundaries of the VP, as defined by the transition from block (A,E) to unidirectional retrograde conduction (B,C,F,G) and the transition from retrograde conduction to bidirectional conduction (D,H). Wavelets (or wave fragments) are the 2D and 3D equivalents of unidirectional conduction.

agreement between theory and data. Figure 7 displays the relationship between the VP and electrode lengths varying from 1.5 mm to 3.9 mm where $g_{Na} = 4 \text{ mS/cm}^2$. Least squares fitting of a linear model yielded a slope of 17.79 ms/cm which should correspond to the reciprocal conduction velocity. The conduction velocity was 56.87 cm/sec and its reciprocal was 17.58 ms/cm, in good agreement with the data.

We next explored the dependence of the vulnerable period on reductions in both the maximum Na conductance, g_{Na} , and use-dependent reductions in Na conductance. Shown in Fig. 8 is a plot of the

vulnerable period as a function of the inverse velocity of the conditioning (s1) wave. Frequency-dependent Na channel blockade produced a linear increase in VP as a function of $1/v$ while reductions in g_{Na} resulted in a nonlinear relationship. Moreover, there was an offset between the frequency-dependent results (+) and reductions in g_{Na} (box) indicating that other factors were significantly altering the VP.

The VP model [Wiener & Rosenbleuth, 1946; Winfree, 1987; Starmer, *et al.*, 1994; Starobin *et al.*, 1994] predicted a linear relationship between VP and stimulus field extent and between VP and the

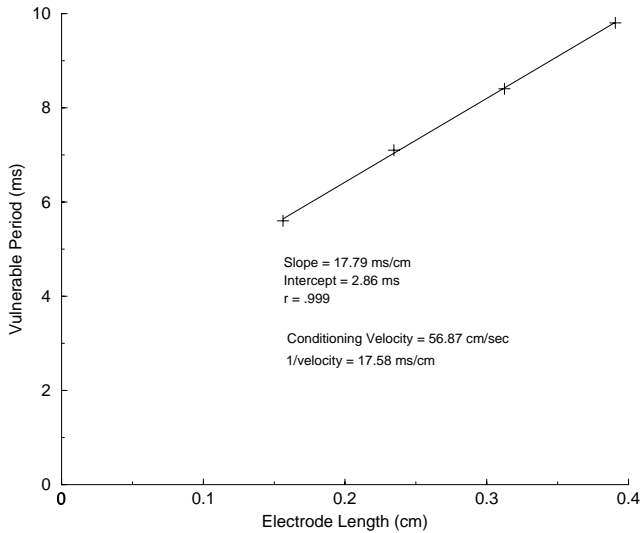


Fig. 7. The sensitivity of the VP — electrode length relationship to the dynamics of Na channel blockade. The stimulus region was varied from 1.5 to 3.9 mm. The conditioning wave velocity was 56.87 cm/sec $g_{Na} = 4$ mS/cm². The least squares slope of the VP — $1/v$ relationship was 17.79 ms/cm, in good agreement with the reciprocal velocity, 17.58 ms/cm.

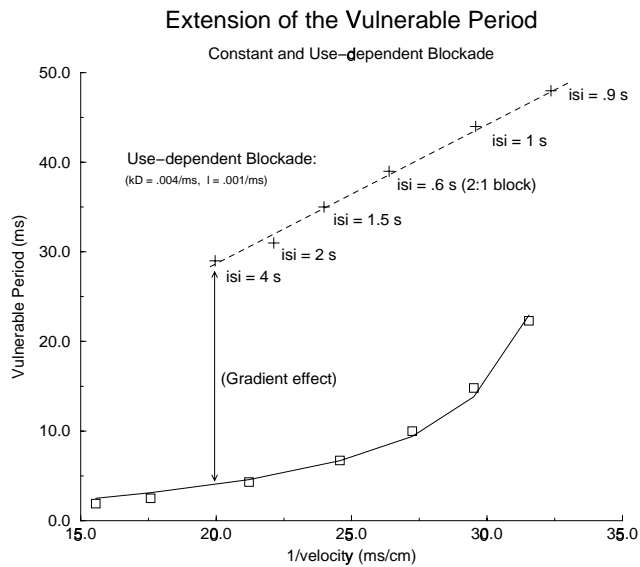


Fig. 8. Variations in the vulnerable period associated with fixed reductions in Na channel availability (reducing g_{Na} , box) and with use-dependent blockade (+). As g_{Na} was reduced, the conduction velocity was similarly reduced and the VP increased in a nonlinear manner. By changing the stimulus interval from 4 s to 600 ms we observed a progressive increase in the VP, but the magnitude was approximately five to seven fold greater than that associated with simply reducing g_{Na} . The dashed line represents the least squares fit of $VP = L/v$ where $1/v$ was the independent variable. The dashed line represents the fit of a linear model ($VP = L/v$) to the frequency-dependent VP measurements. The solid line represents the least squares fit of $VP = [L - (\delta/\nabla A)]/v$ to the data where $\nabla(A)$ and v were the independent variables.

reciprocal conditioning velocity. Thus, the nonlinear relationship between VP and the inverse conditioning velocity was unexpected. These models were based on the assumption that there was a steep transition between excitable and refractory mediums (large gradient). To test this assumption, we presumed that Na channel availability would accurately approximate membrane excitability and plotted the spatial distribution of Na channel availability at the two VP boundaries: the time of the transition from block and retrograde propagation and the time of the transition from retrograde propagation and bidirectional propagation (Fig. 9). We plotted the availability curves for values of g_{Na} ranging from 2 mS/cm² (bottom curve) to 5 mS/cm² (top curve). We identified two critical values of Na availability: one associated with initiation of stable retrograde propagation, P_r , and a larger value associated with initiation of stable antegrade propagation, P_a .

These results revealed that the vulnerable region was sensitive not only by the passage of the critical point over the excitation field, but also to the time required to establish stable propagation in the antegrade direction [compare Figs. 6(C) and 6(G)]. We approximated the extension of the vulnerable region, a virtual electrode of length, L_v , by estimating the time required for the retrograde critical availability, P_r to recover to the antegrade critical value, P_a . Let $\delta = P_a - P_r$ then the distance required to recover this increment of availability is

$$L_v = -\frac{\delta}{\nabla A} \quad (16)$$

where the availability is $A = g_{Na}jh$. Consequently, the VP can be written as

$$VP = \frac{L - \frac{\delta}{\nabla A}}{v} \quad (17)$$

Fitting Eq. (17) (with v and ∇A as independent variables) was in good agreement with the data shown in Fig. 8 (solid line). Given that there is a critical excitability associated with establishing retrograde propagation (unidirectional propagation), then reducing the maximum Na conductance will always reduce the spatial gradient at the critical point, a consequence of moving up the excitability curve towards the plateau (maximum) value.

To be effective, use- and frequency-dependent antiarrhythmic drugs must be characterized by both a rapid rate of binding and a long unbinding

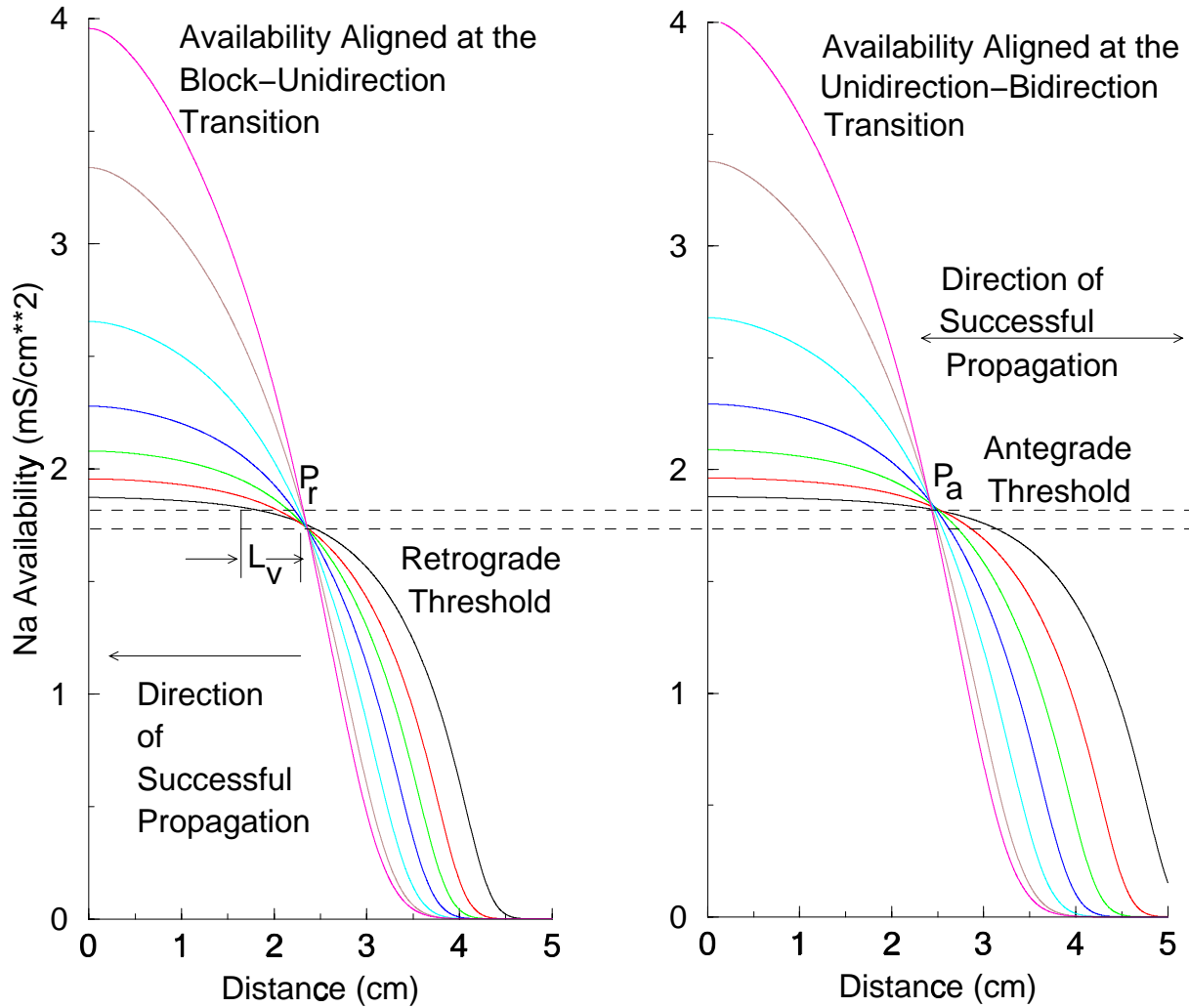


Fig. 9. The spatial distribution of Na channel availability (excitability) trailing the conditioning wave. Shown are superpositions of Na channel availability for values of g_{Na} ranging from 2 to 5 mS/cm² measured at the s1-s2 delay associated with the transition from block to retrograde conduction (left) and retrograde conduction to bidirectional conduction (right). The s2 electrode was located at $x = 2.5$ cm. Each panel displays an intersection, P_r (retrograde conduction) and P_a (antegrade conduction), representing the critical excitability associated with the transition in front development. The asymmetry in propagation development is reflected by $P_r < P_a$ since development of stable retrograde propagation occurs in a region of more recovered medium while development of stable antegrade propagation occurs in a region of less recovered medium.

time constant. Rapidly unbinding drugs would produce only a small, if any, accumulated effect during periodic activation and thus would not significantly prolong the refractory period. The drugs used in the CAST study [CAST, 1989] had time constants exceeding 1 sec (moricizine, $\tau = 1.3$ sec and flecainide, $\tau = 15.5$ sec) [Starmer *et al.*, 1991]. The link between drug unbinding rate, the spatial gradient and altering the vulnerable period can be readily shown.

The gradient of availability in the presence of a channel blocking drug is

$$\nabla A = g_{Na} \frac{db}{dx} = \frac{g_{Na}}{v} \frac{db}{dt} \tag{18}$$

Between heart beats, the Na channel binding sites are not accessible, and thus

$$\frac{db}{dt} = -lb \tag{19}$$

so the gradient at P_r is proportional to the unbinding rate constant:

$$\nabla A = g_{Na} \frac{-lb_{crit}}{v} \tag{20}$$

where b_{crit} is the fraction of blocked channels associated with the critical availability, P_r . Let δ be the difference between the critical antegrade and retrograde availabilities, $A(P_a) - A(P_r)$. Then the

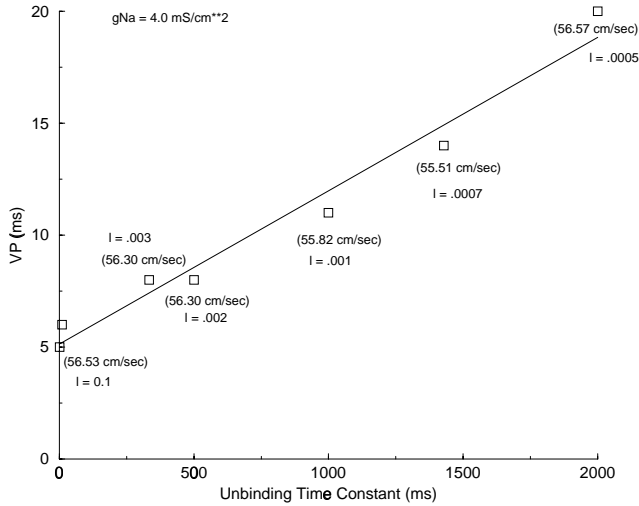


Fig. 10. The VPs computed for different rates of unblock of a use-dependent drug from the Na channel. Drug blockade was modeled as block of inactivated channels with a binding rate of $k[D](1 - h)$ and an unbinding rate of l . Numerically, $k[D] = 0.002$ events/ms and l ranged from 0.0005 events/ms to 0.1 events/ms. The test stimulus was introduced after a single conditioning wave. The conditioning wave velocity was virtually constant (~ 56.5 cm/sec) so that the VP should be constant if there were no gradient effect. There was a four fold increase in the VP as the unbinding rate was reduced from 0.1 to 0.0005, consistent with Eq. (15).

length of the virtual electrode is $-(\delta/\nabla A(x = P_r))$. So the virtual electrode extension is proportional to the unbinding time constant $\tau = 1/l$

$$L_v = -\frac{\delta}{\nabla A(x = P_r)}$$

$$= -\frac{\delta}{\frac{-g_{Na}lb_{crit}}{v}} = \frac{\delta\tau}{g_{Na}b_{crit}v} \quad (21)$$

To test this hypothesis, we computed the VP for drugs with unbinding rates varying from 0.01 (100 ms time constant) to 0.0005 events/ms (2 s time constant) following the first conditioning stimulus (so that the conditioning wave velocity would be relatively constant). As seen in Fig. 10, the VP was linearly related to the unbinding time constant, which is in qualitative agreement with clinical and tissue studies.

The gradient effect provides a basis for interpreting the difference between the linear VP-velocity relationship (Fig. 8) for frequency-

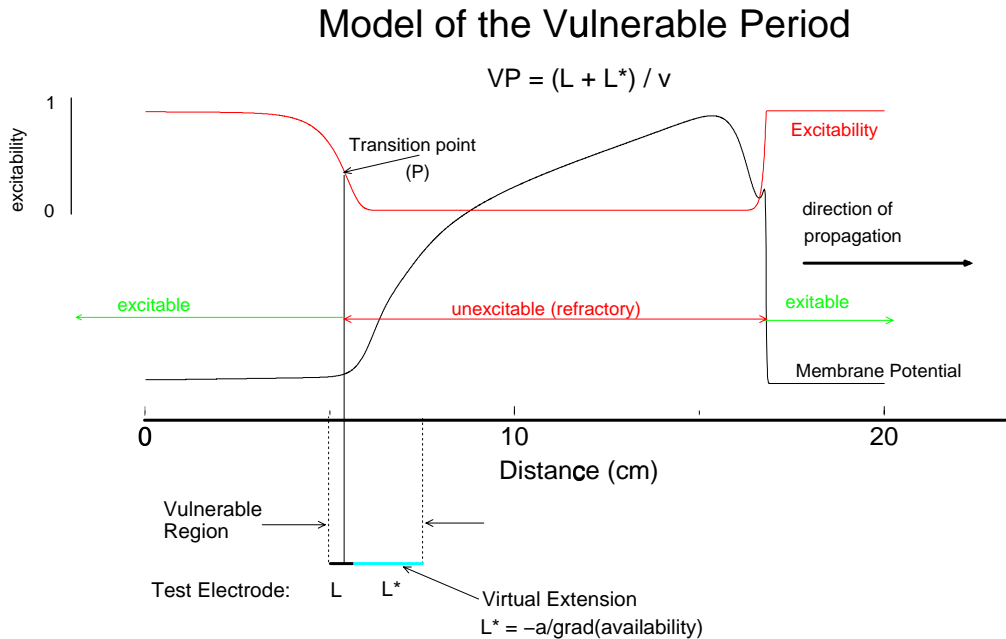


Fig. 11. Model of the vulnerable period. Shown is the spatial distribution of the Na channel availability (excitability) and a propagating action potential. As the critical availability for retrograde propagation, P_r , traverses the s2 electrode, an impulse is formed that extends in the retrograde direction and collapses in the antegrade direction. After P_r passes the end of the physical electrode, antegrade propagation continues to fail due to front extension into less recovered medium. P_r must continue for an additional distance until the critical antegrade availability, P_a arrives at the end of the physical electrode. This additional distance is inversely proportional to the availability gradient and in a marginally excitable medium, can dramatically extend the VP.

dependent blockade and the nonlinear VP-velocity relationship associated with reductions in g_{Na} . All the frequency-dependent measurements of the VP used $g_{\text{Na}} = 4 \text{ mS/cm}^2$. Consequently, any alteration in the availability gradient would be a result of the unbinding kinetics of the drug. Since the rates of drug binding and unbinding were identical for each stimulus rate and the critical excitability exists, then the gradient effect would be independent of the stimulus rate and would lead to a constant virtual extension of the electrode. The result would be a linear relationship between VP and velocity. On the other hand, altering the maximum Na channel availability, g_{Na} , altered the availability gradient as seen in the lower plot in Fig. 9 reflecting alteration in the virtual electrode length. Consequently, the virtual electrode length increased as g_{Na} is reduced, with a concomitant increase in the VP.

With these observations, we refined the original W-R model of vulnerability by incorporating a virtual electrode reflecting the gradient effect. Shown in Fig. 11 is a model of a cardiac action potential, the phase wave of excitability and their relationship to a stimulus field. As the critical point, P_r , passes over the physical electrode field, a retrograde wave is formed that propagates into more excitable medium (to the left). On the other hand, the antegrade wave collapses because the medium to the right has not yet exceeded the threshold for establishing stable antegrade propagation. As P_r continues to pass beyond the right boundary of the physical electrode and across the virtual extension, unstable antegrade wave motion continues to persist until the excitability at the physical electrode boundary reaches the higher threshold, P_a , necessary to support stable propagation into less recovered medium.

7. Discussion

Sanderson [1996] expressed disappointment that drugs showing antiarrhythmic promise when studied in single cells actually increased the incidence of sudden cardiac death when used in patients. It is indeed paradoxical that the same property of a drug that leads to antiarrhythmic responses in isolated cells can become proarrhythmic in a multicellular (whole heart) preparation. Within this setting, it is interesting to note that many abused substances block Na channels and frequently drug-abusers

appear in emergency rooms with re-entrant cardiac arrhythmias, consistent with this property [Whitcomb *et al.*, 1989]. Perhaps this model, linking the cellular antiarrhythmic potential with the multicellular proarrhythmic potential is a candidate for resolving Sanderson's paradox.

To probe the possible links between anti- and pro-arrhythmic processes, we exploited a theoretical model suggested by Wiener and Rosenblueth [1946] and with numerical studies probed the relationship between Na channel availability and the vulnerable period in an homogeneous and continuous medium. These studies were based on the generic property of vulnerability seen not only in cardiac preparations but also in chemical reactions [Gomez-Gesteira *et al.*, 1994].

Earlier in vitro studies with isolated guinea-pig ventricular muscle [Nesterenko *et al.*, 1992] and rabbit isolated left atrium [Starmer *et al.*, 1992] revealed drug-induced prolongation of the VP that was out of proportion to that expected from a reduction in the conduction velocity. In both preparations we found that the VP could be readily extended with drugs that blocked the Na channel. In the guinea-pig studies, under drug-free conditions, we measured a maximum VP of 5 ms. With $1 \mu\text{M}$ moricizine, the VP was extended to 17 ms and increasing the concentration to $12 \mu\text{M}$ extended the VP to 35 ms. Similarly, in the presence of $3 \mu\text{M}$ flecainide (used in the CAST study [CAST Investigators, 1989; CAST II Investigators, 1992]) we measured a VP of 50 ms. Recognizing that many abused substances exhibited Na blocking properties, we tested propoxyphene and cocaine in rabbit atrial tissue [Starmer *et al.*, 1992]. In these studies, the VP under drug-free conditions could not be detected. However, in the presence of $2 \mu\text{M}$ propoxyphene or $1 \mu\text{M}$ cocaine, the VP was greater than 30 ms.

The link between the VP, membrane excitability and its spatial gradients that trail a propagating wave reveals how ion channel blockade can promote simultaneously anti- and pro-arrhythmic properties. Na channel blockade (which reduces excitability and slows the recovery of excitability in individual cells, an antiarrhythmic property) simultaneously, in multicellular preparations, reduces the excitability gradient and extends the period of vulnerability during which unexpected stimuli can initiate unidirectional propagation (by slowing conduction and altering the gradient of excitability). These properties promote wavelet formation which can lead to

spiral waves following premature stimulation. That the gradient of excitability is important has been recently highlighted in studies of defibrillation. Chen *et al.* [1999] and Yamanouchi *et al.* [2001] demonstrated that defibrillation pulse polarity, which alters membrane excitability within the defibrillation field, was linked to defibrillation failure.

In summary, these studies suggest that many of the complexities of a real cardiac cell can be ignored when studying re-entrant arrhythmogenic processes. Altering excitability and the dynamics of the recovery of excitability displays both anti- and pro-arrhythmic effects. Both velocity and spatial gradients of excitability alter the VP. The dominant mechanism of the VP appears to be the interaction between the front formation process in a nonlinear reaction-diffusion medium and the dynamic alteration of the medium's excitability, in this case, with Na channel availability. The mechanism of vulnerability is a generic property of any excitable medium and as such should be the target of intensive investigation.

References

- Allessie, M., Bonke, F. I. M. & Schopman, J. G. [1973] "Circus movement in rabbit atrial muscle as a mechanism of tachycardia," *Circ. Res.* **33**, 54–62.
- Beeler, G. W. & Reuter, H. [1977] "Reconstruction of the action potential of ventricular myocardial fibers," *J. Physiol. London* **268**, 177–210.
- Cardiac Arrhythmia Suppression Trial Investigators [1989] "Preliminary report: Effect of encainide and flecainide on mortality in a randomized trial of arrhythmia suppression after myocardial infarction," *New Eng. J. Med.* **321**, 406–412.
- Cardiac Arrhythmia Suppression Trial-II Investigators [1992] "Effect of the antiarrhythmic agent moricizine on survival after myocardial infarction," *N. Eng. J. Med.* **327**, 227–233.
- Cheng, Y., Mowrey, A., VanWagoner, D. R., Tchou, P. J. & Efimov, I. R. [1999] "Virtual electrode-induced re-excitation: A mechanism of defibrillation," *Circ. Res.* **85**, 1056–1066.
- Ferris, L. P., King, B. G., Spence, P. W. & Williams, B. H. [1936] "Effect of electric shock on the heart," *Elect. Engin.* **55**, 489–515.
- FitzHugh, R. [1961] "Impulses and physiologic states in theoretical models of nerve membrane," *Biophys. J.* **1**, 445–466.
- Gilliam, F. R., Starmer, C. F. & Grant, A. O. [1989] "Blockade of rabbit atrial sodium channels by lidocaine: Characterization of continuous and frequency-dependent blocking," *Circ. Res.* **65**, 723–739.
- Gomez-Gesteira, M., Fernandex-Garcia, G., Munuzuri, A. P., Perez-Munuzuri, V., Krinsky, V. I., Starmer, C. F. & Perez-Villar, V. [1994] "Vulnerability in excitable Belousov-Zhabotinsky medium: From 1 D to 2 D," *Physica* **D76**, 359–368.
- Heistracher, P. [1971] "Mechanism of action of antiarrhythmic drugs," *Naunym-Schmiedebers Arch. Pharmacol.* **269**, 199–211.
- Hodgkin, A. L. & Huxley, A. F. [1952] "A quantitative description of membrane current and its application to conduction and excitation in nerve," *J. Physiol. Lond.* **177**, 500–544.
- Johnson, E. A. & McKinnon, M. G. [1957] "The differential effect of quinidine and pyralamine on the myocardial action potential at various rates of stimulation," *J. Pharmacol. Exp. Ther.* **120**, 460–568.
- Krinsky, V. I. [1966] "Spread of excitation in an inhomogeneous medium (state similar to cardiac fibrillation)," *Biofizika* **11**, 676–683.
- Lou, C. & Rudy, Y. [1991] "A model of the ventricular action potential: Depolarization, repolarization and their interaction," *Circ. Res.* **68**, 1501–1526.
- Nesterenko, V. V., Lastra, A. A., Rosenstraukh, L. V. and Starmer, C.F. [1992] "A proarrhythmic response to Na channel blockade: Prolongation of the vulnerable period in guinea-pig ventricular myocardium," *J. Cardiol. Pharm.* **19**, 810–820.
- Sanderson, J. [1996] "The sword of Damocles," *Lancet* **348**, 2–3.
- Starmer, C. F. & Grant, A. O. [1985] "Phasic ion channel blockade: A kinetic model and parameter estimation procedure," *Mol. Pharmacol.* **28**, 348–356.
- Starmer, C. F. [1988] "Characterizing activity-dependent processes with a piecewise exponential model," *Biometrics* **44**, 549–559.
- Starmer, C. F., Nesterenko, V. V., Undrovinas, A. I., Grant, A. O. & Rosenshtraukh, L. V. [1991a] "Lidocaine blockade of continuously and transiently accessible sites in cardiac sodium channels," *J. Mol. Cell. Cardiol.* **23**, 73–83.
- Starmer, C. F., Lastra, A. A., Nesterenko, V. V. & Grant, A. O. [1991b] "Proarrhythmic response to sodium channel blockade: Theoretical model and numerical experiments," *Circulation* **84**, 1364–1377.
- Starmer, C. F., Lancaster, A. R., Lastra, A. A. & Grant, A. O. [1992] "Cardiac instability amplified by use-dependent Na channel blockade," *Amer. J. Physiol.* **262**, H1305–H1319.
- Starmer, C. F., Biktashev, V. N., Romashko, D. N., Stepanov, M. R., Makarova, O. N. & Krinsky, V. I. [1994] "Vulnerability in an excitable medium: Analytical and numerical studies of initiating unidirectional propagation," *Biophysical J.* **65**, 1775–1787.
- Starobin, J., Zilberter, Y. I. & Starmer, C. F. [1994] "Vulnerability in one-dimensional excitable media," *Physica* **D70**, 321–341.

- Whitcomb, D. C., Gilliam, F. R., Starmer, C. F. & Grant, A. O. [1989] "Marked QRS complex abnormalities and sodium channel blockade by propoxyphene reversed with lidocaine," *J. Clin. Invest.* **84**, 1929–1936.
- Wiener, N. & Rosenblueth, W. [1946] "The mathematical formulation of the problem of conduction of impulses in a network of connected excitable elements, specifically in cardiac muscle," *Arch. Inst. Cardiol. Mex.* **16**, 205–265.
- Wiggers, C. J. & Wegria, R. [1939] "Ventricular fibrillation due to single localized induction and condenser shocks applied during the vulnerable phase of ventricular systole," *Amer. J. Physiol.* **128**, 500–505.
- Winfrey, A. T. [1987] *When Time Breaks Down* (Princeton University Press, NJ).
- Yamanouchi, Y., Cheng, Y., Tchou, P. J. & Efimov, I. R. [2001] "The mechanisms of the vulnerable window: The role of virtual electrodes and shock polarity," *Can. J. Physiol. Pharmacol.* **79**, 25–33.
- Zilberter, Y. I., Starmer, C. F. & Grant, A. O. [1994] "Open Na channel blockade: Multiple rest states revealed by channel interactions with disopyramide and quinidine," *Amer. J. Physiol.* **266**, H2007–H2017.